

Interface effects in *d*-wave superconductor-ferromagnet junctions in the vicinity of domain walls

T. Kirzhner and G. Koren

Physics Department, Technion-Israel Institute of Technology, Haifa 32000, Israel

(Received 1 June 2010; revised manuscript received 7 September 2010; published 5 October 2010)

Measurements of the differential conductance spectra of $\text{YBa}_2\text{Cu}_3\text{O}_{7-\delta}\text{-SrRuO}_3$ and $\text{YBa}_2\text{Cu}_3\text{O}_{7-\delta}\text{-La}_{0.67}\text{Ca}_{0.33}\text{MnO}_3$ ramp-type junctions along the node and antinode directions are reported. Interpretation of the results in terms of crossed Andreev reflection effect and induced triplet superconductivity are discussed. The results are consistent with a crossed Andreev reflection effect only in $\text{YBa}_2\text{Cu}_3\text{O}_{7-\delta}\text{-SrRuO}_3$ junctions where the domain-wall width of SrRuO_3 is comparable with the coherence length of $\text{YBa}_2\text{Cu}_3\text{O}_{7-\delta}$. No such effect was observed in the $\text{YBa}_2\text{Cu}_3\text{O}_{7-\delta}\text{-La}_{0.67}\text{Ca}_{0.33}\text{MnO}_3$ junctions, which is inline with the much larger ($\times 10$) domain-wall width of $\text{La}_{0.67}\text{Ca}_{0.33}\text{MnO}_3$. We also show that crossed Andreev exists only in the antinode direction. Furthermore, we find evidence that crossed Andreev in $\text{YBa}_2\text{Cu}_3\text{O}_{7-\delta}$ junctions is not sensitive to nanometer-scale interface defects, suggesting that the length scale of the crossed Andreev effect is larger than the coherence length, but still smaller than the $\text{La}_{0.67}\text{Ca}_{0.33}\text{MnO}_3$'s domain-wall width.

DOI: 10.1103/PhysRevB.82.134507

PACS number(s): 74.45.+c, 75.70.-i, 74.50.+r

The proximity effect between a ferromagnet (F) and a superconductor (S) has attracted much attention in the past few years. Many scattering processes can occur at the S-F interface and a full understanding of these effects is still lacking. One such process is the nonlocal crossed Andreev reflection effect (CARE), where an incident electron is reflected as a hole into a spatially separated electrode while a Cooper pair is created in the superconductor.¹ In this process the electron and hole remain in an entangled coherent state as long as they do not scatter inelastically. Another possible process is the proximity-induced triplet superconductivity (PITS) in F in the vicinity of inhomogeneities.^{2,3} The CARE process can be detected experimentally by measuring the conductance of spatially separated normal-metal (N) or F electrodes coupled to a superconductor while the PITS process can be measured only in S-F contacts. Previous studies show that CARE is possible only when the spatial separation of the metallic electrodes is on the order of the superconducting coherence length ξ_S .⁴ Both CARE and PITS can exist in the vicinity of domain walls (DWs) in S-F junctions. CARE seems to occur as long as the DW width is comparable to ξ_S ,⁵⁻⁷ while the existing theories for PITS do not necessitate such a stringent requirement.^{3,8}

Since CARE is a spin-dependent process, half-metal ferromagnetic leads with nonzero spin polarization can cause favoring of the CARE process under certain conditions.⁹ In the case of fully polarized ferromagnetic leads with antiparallel spin configuration, spin-up electrons in one electrode can be reflected as spin-down holes in the other electrode, allowing CARE, while in the case of parallel spin configuration, CARE cannot exist. It was shown that the DW structure of a ferromagnet can greatly modify the proximity effect of an S-F system.^{6,7} CARE effect is expected when the ferromagnet DW width is of the same order of magnitude as ξ_S , where nonlocal Andreev reflection is possible. When the ferromagnet is not fully polarized, local Andreev reflection is also possible and contributes to the junction conductance.

To this day, most of the research related to CARE and PITS was focused on the case of *s*-wave superconductors. In the case of *d*-wave superconductors, better understanding is still needed. These cases were discussed theoretically by

Herrera *et al.*¹⁰ and by Volkov and Efetov,¹¹ but only a few experimental studies had been reported.^{6,7} In Ref. 10, several unique properties of CARE were investigated in the configuration of two metal electrodes in contact with a *d*-wave superconductor. Surprisingly, it was found that CARE is a long-range effect in *d*-wave superconductors and can occur with electrode separation of up to $\sim 5\xi_S$, as opposed to only $\sim \xi_S$ in *s*-wave superconductors. In addition, the angular dependence of CARE was found to be strongest in the antinode direction.

In this study we investigate signatures of CARE and PITS effects in *d*-wave superconductors by using high-quality ferromagnet—*d*-wave superconductor (F-S) ramp-type junctions with *a*-*b* plane coupling [see inset (b) of Fig. 1]. We prepared various configurations of ramp junctions containing optimally doped $\text{YBa}_2\text{Cu}_3\text{O}_{7-\delta}$ (YBCO) as the *d*-wave superconductor and two different types of ferromagnets: SrRuO_3 (SRO) and $\text{La}_{0.67}\text{Ca}_{0.33}\text{MnO}_3$ (LCMO). The junctions were prepared along two different angular orientations, in the node and antinode directions. SRO and LCMO have been chosen as the ferromagnetic electrodes to investigate the DW width

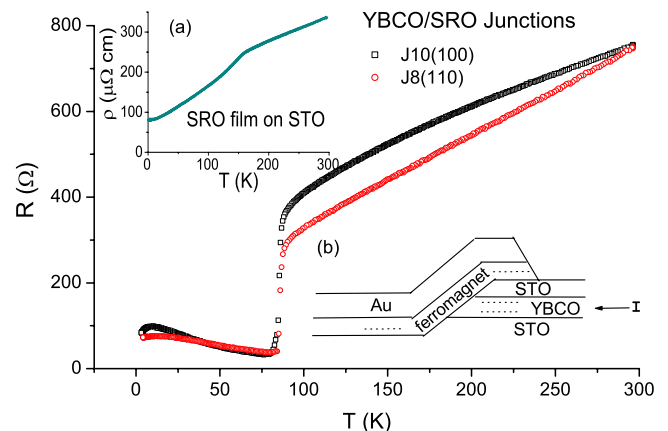


FIG. 1. (Color online) Resistance versus temperature of YBCO-SRO junctions along the node (squares) and antinode (circles) orientations. Insets: (a) ρ versus T of a bare SRO film on (100) STO. (b) A schematic ramp junction cross section.

dependence of the studied effects. The DW width in SRO is $\sim 2\text{--}3$ nm (Refs. 12 and 13) which is comparable to $\xi_S \sim 2\text{--}3$ nm of YBCO. LCMO has a much larger DW width, in the range of 20–40 nm at the low-temperature regime.^{14,15} Typical domain widths of SRO and LCMO are of about 200 nm and 300 nm, respectively.^{12,14} It was also found in these studies that the DW orientations of *c*-axis grown SRO and LCMO films on (100) SrTiO₃ (STO) are along the (110) and (100) directions, respectively. If we assume similar DW orientations when grown on twinned *c*-axis YBCO, this corresponds to the nodes and antinodes directions. This leads to many domain-wall crossings of the interface in our 5 μm wide junctions (about 18 and 15 crossings in the antinode junctions with SRO and LCMO, respectively, with the corresponding values of 25 and 11 in the node-oriented junctions). We found that the differential conductance spectra of these junctions provide evidence for the long-range nature of the CARE effect and agree well with the theoretical predictions of the angular dependence of this effect.¹⁰ Within the framework of the existing theories for PITS, no agreement with the detailed experimental data was found.

A schematic of a typical ramp junction is shown in inset (b) of Fig. 1. These junctions were prepared by a multistep process. The films were prepared by laser ablation deposition, patterning was done by a waterless resist and deep UV photolithography and etching by Ar-ion milling. Antinode (100) and node (110) oriented junctions were obtained by depositing *c*-axis YBCO films on (100) STO wafers of 10×10 mm² area, with their sides parallel to either the (100) or (110) orientations, respectively. The detailed preparation process is described elsewhere,¹⁶ and here we shall only briefly summarize the main steps. First, the base electrode was deposited which include a 60 nm layer of STO on top of an 80-nm-thick YBCO film. This bilayer was patterned on half of the wafer into ten 15- μm -wide bridges with a ramp angle of $\sim 35^\circ$, and connections to the contact pads. The cover electrode was deposited next and included either SRO or LCMO layers of 20 nm thickness capped with an 80 nm thick gold layer for the leads and contacts. Then the final patterning produced ten separated junctions of 5 μm width on the wafer with four contacts each. Overall, in the present study 12 such wafers were prepared with the results being reproducible in at least three junctions of each orientation and type.

Figure 1 shows the R versus T curves of the YBCO-SRO junctions. Inset (a) of this figure shows the ρ versus T of a bare SRO film on (100) STO where a clear signature of the ferromagnetic transition at 150 K can be seen. It is hard to notice this transition temperature in the main panel at around 150 K due to the low SRO film resistance (20 nm thickness and $\rho \sim 0.5$ m Ω cm) compared to that of YBCO (80 nm thickness and $\rho \sim 1.5$ m Ω cm). The low-temperature resistance of these junctions (~ 100 Ω) is much higher than that of the bare SRO films. The origin of this interface resistance therefore, is apparently due to exposure of the ramps to ambient air before the deposition of the cover electrode. Figure 2 shows typical R versus T curves of the YBCO-LCMO junctions in the main panel together with the ρ versus T data of a bare LCMO film on (100) STO in the inset. The resistance curves have a broad maximum at around 110–180 K,

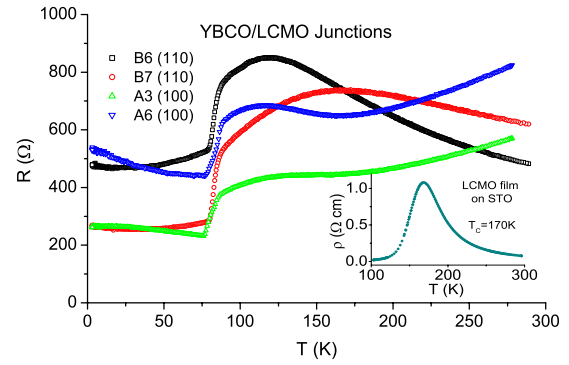


FIG. 2. (Color online) Resistance versus temperature of YBCO-LCMO junctions along the node (squares and circles) and antinode (up and down triangles) orientations. Inset: ρ versus T of a bare LCMO film on (100) STO.

which indicates the transition temperature to ferromagnetism T_c of the LCMO layer. At low temperatures, the junctions have resistances of 200–600 Ω which are much higher than the typical LCMO film resistance (see the inset of Fig. 2). Similarly to the SRO case, it is due to the formation of a more resistive layer at the interface.

Figure 3(a) shows three normalized differential conductance spectra of (100) oriented YBCO-SRO junctions at zero magnetic field. One, after zero-field cooling and the other two, after applying fields of ± 5 T in a direction perpendicular to the CuO₂ planes of YBCO. The conductance spectra show a clear zero bias conductance peak (ZBCP) superposed on a parabolic background. As shown by Tanaka and Kashiwaya¹⁷ for a *d*-wave superconductor, the ZBCP is a result of Andreev bound states near zero bias which are formed in the (110) (node) direction of the N-S junctions while a tunneling gap is expected in the (100) (antinode) direction. Many theoretical and experimental results however,^{18–21} show that a ZBCP can also be formed in the (100) direction, due to nanometer-scale interface roughness, and that its strength can be comparable to that of a ZBCP formed with a perfect (110) interface. Using atomic force microscopy imaging of the ramp (interface) of our junctions, we found that the surface roughness is of about $\sim 1\text{--}3$ nm, with no grain boundaries. This indicates that the ZBCP we observed might originate in the node bound states due to the interface roughness. Control experiments made with YBCO-Au junctions oriented in the (100) and (110) directions, showed ZBCPs with comparable strength in both orientations, strengthening the assumption that nanometer-scale roughness can lead to their formation.

As discussed before, the conductance of a superconductor coupled to partially polarized ferromagnetic electrodes, has contributions of both local and nonlocal AR effects. SRO in the ferromagnetic state has spin polarization of about 50%,²² thus local AR is also possible. Since the domains width size (~ 200 nm) is so much larger than the DW width (~ 3 nm), the domain-walls configuration should not affect the junction conductance originated from local AR. To detect only the CARE effect, we investigated how the domain-wall structure affects the junction conductance by application of various magnetic fields. Magnetic fields of ± 5 T, which are

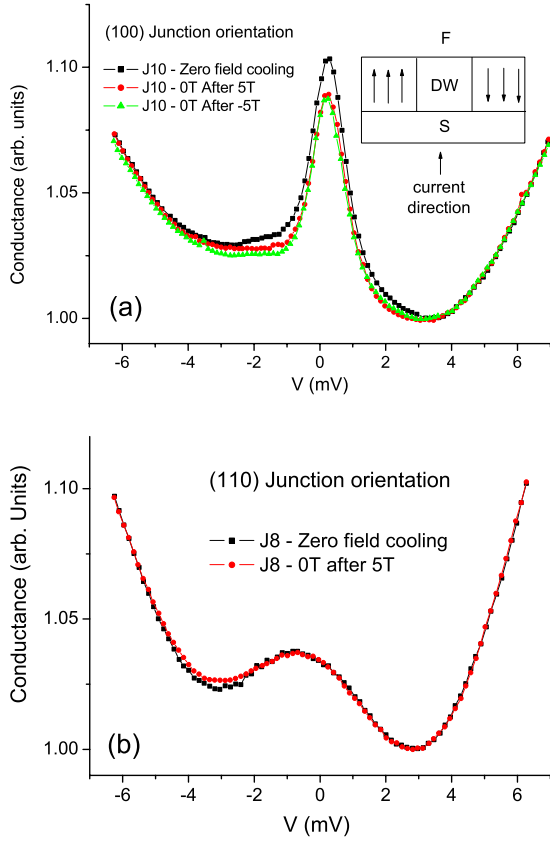


FIG. 3. (Color online) Conductance spectra at zero field of (a) (100) and (b) (110) oriented YBCO-SRO junctions. The squares represent the zero-field cooling spectra while the circles and triangles spectra show the results after field cycling to +5 T and -5 T, respectively. Inset: the ferromagnet DW geometry in our S-F junctions.

much higher than the coercive fields of both SRO (0.5 T) (Ref. 23) and LCMO (0.05 T) (Ref. 15) were applied, to make sure that the domain structure in the ferromagnetic electrodes is changed. Hysteresis of the ZBCP height can be seen in Fig. 3(a) after application of these magnetic fields and returning to zero field. This leads to a reduction in the ZBCP height by $\sim 15\%$, after this field cycling process. A similar behavior was also seen previously by Aronov and Koren⁶ in (100) oriented S-F-S and S-F junctions. To understand this behavior, we note that in zero-field cooling of the ferromagnet, many domains and domain walls are formed. Clearly, after the magnetic field cycling as described above, the ferromagnet is much more oriented and the number of domain walls is significantly decreased. Considering the fact that the SRO DW width is comparable to the superconducting coherence length of YBCO, a large number of domain walls crossing the interface in S-F junctions should enhance the CARE conductance. This agrees well with the present results of our measurements.

It is well known that strong magnetic fields can also cause suppression and/or splitting of the ZBCP.¹⁸ The observed decrease in the junction conductance after field cycling therefore, could be affected by the ferromagnet's remanent magnetization field. This however is not the case, since the stray magnetic field emanating from the SRO crystallites of

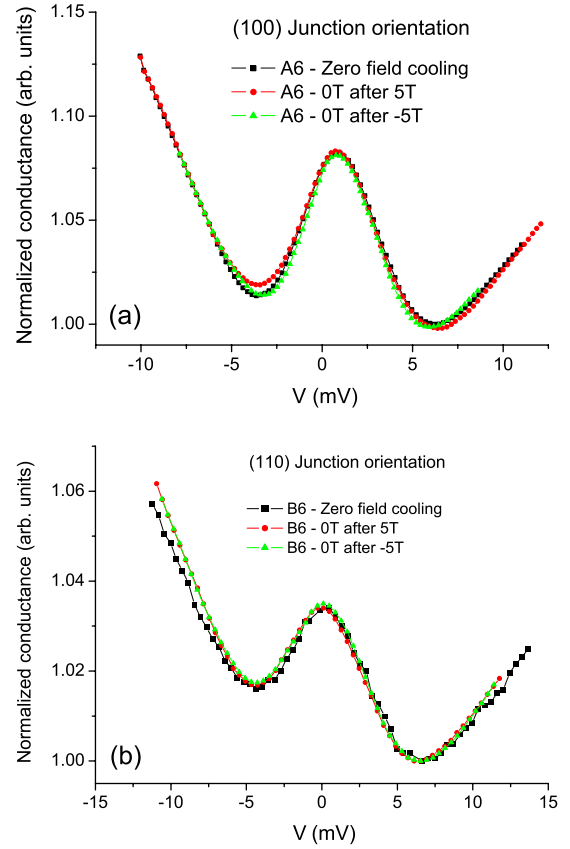


FIG. 4. (Color online) Normalized zero-field conductance spectra of (a) (100) and (b) (110) oriented YBCO-LCMO junctions, under zero-field cooling and after field cycling to ± 5 T and back to zero field.

~ 0.2 T (Ref. 23) is too weak to cause this effect. This was confirmed in conductance measurement of the YBCO-Au junctions, where a very little change in the ZBCP conductance was observed after the application of a 0.2 T field.

Figure 3(b) shows conductance measurement results made on a typical (110) oriented YBCO-SRO junction. No conductance hysteresis after field cycling is found in this case, which is in contrast to the results observed in the (100) junction of Fig. 3(a). According to Ref. 10, in a *d*-wave superconductor, CARE is strongest along the antinode directions where the order parameter amplitude reaches its maximum value. This prediction agrees well with our results. Our results show that CARE which is a nonlocal AR effect, has angular dependence, in contrast to the local AR which is isotropic and does not have angular variations. Considering the interface roughness argument that was made above, one would expect that the conductance increase due to CARE in the (100)- and (110)-oriented junctions should be similar, as in the case of local AR. However, since this conjecture is contrary to the present observations, it is suggested that CARE is not affected by nanometer-scale roughness of the junctions interface. This seems to indicate that long-range CARE correlations in YBCO which is a *d*-wave superconductor, are responsible for the present results and are inline with the theoretical predictions.¹⁰

Figure 4 shows conductance spectra results taken in

(100)- and (110)-oriented YBCO-LCMO junctions. The conductance curves had to be normalized because of the high magnetoresistance of LCMO. The curves were normalized by division of the data by the global minima value of each plot, to allow for a convenient way to compare the ZBCP heights. Normalization by subtraction of the global minima value of each plot was also tried and yielded similar results (not shown). No hysteresis after field cycling can be noticed in the ZBCPs height of any of the YBCO-LCMO junctions. Considering that the LCMO DW width is much larger than the coherence length of the superconductor ξ_S , this result strengthens our argument that the hysteresis effect of the ZBCP height after field cycling seen in Fig. 3(a) is due to CARE contribution rather than to other effects.

We shall now discuss our data in terms of PITS, the proximity-induced triplet superconductivity scenario. Bergeret *et al.*² have found that local inhomogeneities in the magnetization of a ferromagnet in close proximity to a superconductor could induce a triplet superconductive component inside the ferromagnet. This triplet component leads to a long-range proximity effect in F-S junctions and thereby increase their conductance for any given barrier thickness. Local magnetization inhomogeneities are naturally created in ferromagnets by the formation of domains and domain walls. These domain walls could theoretically induce triplet superconductivity in the ferromagnet and therefore increase the junctions conductance. Our measurement results could thus be interpreted in the framework of proximity-induced triplet superconductivity. In the (100)-oriented YBCO-SRO junctions of Fig. 3(a) we found that the conductance increases with the number of domain walls. A large number of domain walls thus leads to many local inhomogeneities in the magnetization, and this induces the triplet condensate component in their vicinity. In our junctions geometry [see inset of Fig. 3(a)], theoretical calculations of a singlet *s*-wave superconductor—ferromagnet junction show that the induced triplet superconductive order in the ferromagnet persists even if the DW width is much larger than the superconducting coherence length.^{3,8} This prediction however, is in contrast to our observations in the YBCO-LCMO junctions, where the number of broad domain walls did not affect the junction conductance as can be seen in Fig. 4. This indicates that either the junction conductance in our case is not affected by triplet superconductivity or that it is affected by triplet superconductivity but the DW width is an important factor in the junction conductance. The latter case is supported by our observations in YBCO-SRO junctions where the conductance is enhanced with increasing number of narrow domain walls, as seen in Fig. 3(a).

Since in the present study a *d*-wave superconductor was used, it is more appropriate to compare our results with the theoretical treatment of Volkov and Efetov.¹¹ They considered an S-F bilayer with S being a *d*-wave superconductor with the *a-b* planes parallel to the interface, *c* axis in the direction of the domain walls in F and the current flowing along the *c*-axis direction. The current in our junctions flows

mostly along the *a-b* planes but due to the ramp angle a small current component also flows in the *c*-axis direction and this allows a comparison with the results of Ref. 11. This paper predicts a maximal long-range triplet component if the DW planes lie in the antinode direction while no triplet component exists if the DW planes lie in the node direction. In the LCMO junctions the DW lie in the antinode directions and thus a maximal triplet-induced component is expected. This should lead to a decrease in the low-bias conductance after magnetic field cycling due to the expected decrease in the number of DW. Figure 4 shows that no such effect occurs. In the SRO junctions the DW lie in the node direction and the model predicts that no triplet component should exist. Field cycling therefore should not affect the observed conductance in this case and this is contrary to our observations [see Fig. 3(a)]. We thus conclude that in both type of junctions, when there is a current component flowing in the *c*-axis direction, the model results disagree with the experimental results. This model however, might be more suitable to describe the present observations if calculations were made with the current flowing in the *a-b* plane. To summarize, while a proximity-induced odd frequency triplet *s*-wave component in the ferromagnets can explain the enhancement of conductance at low bias (the ZBCP) as seen in the experiments, the existing theories cannot account for the DW width dependence of the present results. The CARE based interpretation however seems more suitable since it agrees well with all the current results and shows the correct dependence on the DW widths.

In conclusion, we have found evidence for the existence of a CARE effect in S-F junctions with the *d*-wave superconductor YBCO but proximity-induced triplet superconductivity is also consistent with some of our results. Only when the DW width was comparable to the superconductor coherence length such as in the case of the YBCO-SRO junctions, the low-bias junction conductance was found to be affected by the number of the domain walls in the ferromagnet. In contrast, when the DW width was much larger than the superconductor coherence length such as in the YBCO-LCMO junctions, no effect on the junction conductance was observed. These results can be interpreted as due to CARE with a CARE length scale on the order of the superconducting coherence length. We observed that this effect is not affected by nanometer-scale interface roughness, suggesting that it can also happen on length scales larger than the superconductor coherence length. Moreover, we can put an upper bound on this length scale which is found to be smaller than the DW width of LCMO ($\sim 10\xi_S$). Finally, we also show that the conductance change after magnetic field cycling appears only in the (100) direction suggesting that CARE in a *d*-wave superconductors is angle dependent.

We thank O. Millo for useful discussions. This research was supported in part by the Israel Science Foundation, the joint German-Israeli DIP project, and the Karl Stoll Chair in advanced materials.

- ¹J. M. Byers and M. E. Flatté, *Phys. Rev. Lett.* **74**, 306 (1995).
- ²F. S. Bergeret, A. F. Volkov, and K. B. Efetov, *Phys. Rev. Lett.* **86**, 4096 (2001).
- ³A. F. Volkov, Ya. V. Fominov, and K. B. Efetov, *Phys. Rev. B* **72**, 184504 (2005).
- ⁴G. Deutscher and D. Feinberg, *Appl. Phys. Lett.* **76**, 487 (2000).
- ⁵R. Mélin and S. Peysson, *Phys. Rev. B* **68**, 174515 (2003).
- ⁶P. Aronov and G. Koren, *Phys. Rev. B* **72**, 184515 (2005).
- ⁷I. Asulin, O. Yuli, G. Koren, and O. Millo, *Phys. Rev. B* **74**, 092501 (2006).
- ⁸J. N. Kupferschmidt and P. W. Brouwer, *Phys. Rev. B* **80**, 214537 (2009).
- ⁹D. Beckmann, H. B. Weber, and H. v. Löhneysen, *Phys. Rev. Lett.* **93**, 197003 (2004).
- ¹⁰W. J. Herrera, A. Levy Yeyati, and A. Martín-Rodero, *Phys. Rev. B* **79**, 014520 (2009).
- ¹¹A. F. Volkov and K. B. Efetov, *Phys. Rev. Lett.* **102**, 077002 (2009).
- ¹²A. F. Marshall, L. Klein, J. S. Dodge, C. H. Ahn, J. W. Reiner, L. Mieville, L. Antognazza, A. Kapitulnik, T. H. Geballe, and M. R. Beasley, *J. Appl. Phys.* **85**, 4131 (1999).
- ¹³M. Feigensohn, L. Klein, J. W. Reiner, and M. R. Beasley, *Phys. Rev. B* **67**, 134436 (2003).
- ¹⁴S. J. Lloyd, N. D. Mathur, J. C. Loudon, and P. A. Midgley, *Phys. Rev. B* **64**, 172407 (2001).
- ¹⁵M. Ziese, S. P. Sena, and H. J. Blythe, *J. Magn. Magn. Mater.* **202**, 292 (1999).
- ¹⁶O. Neshet and G. Koren, *Appl. Phys. Lett.* **74**, 3392 (1999).
- ¹⁷Y. Tanaka and S. Kashiwaya, *Phys. Rev. Lett.* **74**, 3451 (1995).
- ¹⁸M. Fogelström, D. Rainer, and J. A. Sauls, *Phys. Rev. Lett.* **79**, 281 (1997).
- ¹⁹M. Covington, M. Aprili, E. Paraoanu, L. H. Greene, F. Xu, J. Zhu, and C. A. Mirkin, *Phys. Rev. Lett.* **79**, 277 (1997).
- ²⁰R. Krupke and G. Deutscher, *Phys. Rev. Lett.* **83**, 4634 (1999).
- ²¹H. W. Cheng, B. C. Yao, C. C. Chi, and M. K. Wu, *Physica C* **341**, 2159 (2000).
- ²²B. Nadgorny, M. S. Osofsky, D. J. Singh, G. T. Woods, R. J. Soulen, M. K. Lee, S. D. Bu, and C. B. Eom, *Appl. Phys. Lett.* **82**, 427 (2003).
- ²³L. Klein, J. S. Dodge, T. H. Geballe, A. Kapitulnik, A. F. Marshall, L. Antognazza, and K. Char, *Appl. Phys. Lett.* **66**, 2427 (1995).